The Use of Atomic Force Microscopy for the Observation of Corneal Epithelium Surface

Miltiadis K. Tsilimbaris,[1] *Eric Lesniewska,*[2] *Stella Lydataki,*[1] *Christian Le Grimellec,*[3] *Jean P. Goudonnet,*[2] *and Ioannis G. Pallikaris*[1]

Purpose. To evaluate the feasibility of imaging normal corneal epithelium by means of atomic force microscopy (AFM).

Methods. Twelve normal corneas from six albino rabbits were examined using a commercial atomic force microscope. Six corneas were examined in balanced salt solution after fixation in glutaraldehyde 2.5% and six without any fixation. Rectangular silicon nitride cantilevers with a spring constant of 10 to 20 mN/m were used. The measured forces after imaging were less than 100 pN. All reported images were made with 512 × 512-pixel definition with typical scan rates ranging from 1 to 5 Hz.

Results. High-quality images of corneal epithelium surface were obtained from fixed and unfixed specimens in magnifications ranging from ×2000 to ×2,000,000. Imaging of fixed specimens was always easier. In unfixed specimens fuzzy images were very common, probably because of the presence of the cell glycocalyx. AFM revealed the typical polygonal corneal epithelial cells. The cell surface was covered by microprojections; at cell borders the microprojections were arranged in two characteristic parallel rows. Craterlike formations were revealed in several specimens. The microprojections' morphology and their surface details were revealed using magnifications up to ×2,000,000. Three-dimensional representation of the images facilitated better understanding of the surface topography. Measurements in horizontal and vertical plane were made using the section analysis tool.

Conclusions. In this work the AFM parameters appropriate for corneal epithelium imaging in physiological medium were defined. AFM represents a new powerful tool for corneal epithelium imaging, and its application in this field warrants further investigation. (*Invest Ophthalmol Vis Sci.* 2000;41:680–686)

The atomic force microscope (AFM) is a recently developed scanning probe microscope that allows noninvasive examination of specimens in their ambient conditions after minimal preparation. In this type of microscopy a sharp probe is brought in proximity to the specimen and is guided over the specimen surface, using force fields between the probe and the sample. The result is a three-dimensional relief of the sample that reflects the nature of the local interaction between the probe and the sample.[1] The great advantage of AFM compared with conventional scanning electron microscopy (SEM) is its ability to obtain topographic information from the specimen surface in aqueous, nonaqueous, or dry conditions. This permits observation of the specimen in conditions close to its normal environment. At the same time, all the preparation necessary for conventional scanning microscopy is avoided. AFM images have a resolution comparable to or even greater than SEM images.[2]

Many biologic specimens, from cells to individual molecules, have been imaged using AFM. Examples include chromosomal DNA, plasmid DNA, proteins, a variety of membranes, and living cells.[3–8] There are only a few published papers related to AFM of eye tissues.[9,10] In the current work we studied the feasibility of imaging the corneal epithelium of normal albino rabbits by means of AFM.

Methods

We used six normal albino rabbits with body weight ranging from 3 to 4 kg. The animals were housed individually in a 12-hour light–12-hour dark cycle and had free access to food and water. They were used in accordance with the ARVO Statement for the Use of Animals in Ophthalmic and Vision Research.

Animals were killed by an injected overdose of pentobarbital sodium delivered through a peripheral ear vein. Immediately after death, the eyes were enucleated carefully to avoid contamination of the corneal surface by blood and to avoid touching the specimen's surface at any time before AFM ex-

From the [1]University of Crete Medical School, Department of Ophthalmology, Heraklion, Greece; [2]University of Bourgogne, Physics Laboratory, Dijon, France; [3]University of Montpellier, Institut National de la Santé et de la Recherche Médicale U414, France.

Presented in part at the annual meeting of the Association for Research in Vision and Ophthalmology, Fort Lauderdale, Florida, May 1997.

Supported by grants from Region Bourgogne, France, and from the University of Crete, Greece.

Submitted for publication January 12, 1999; revised September 2, 1999; accepted September 23, 1999.

Commercial relationships policy: N.

Corresponding author: Miltiadis K. Tsilimbaris, Lecturer in Ophthalmology, University of Crete Medical School, PO Box 1352, Heraklion, Crete, GR 711 10, Greece. tsilimb@med.uoc.gr

Copyright © Association for Research in Vision and Ophthalmology

amination. One eye was put in a moisture chamber and the other in fixative solution (glutaraldehyde 2.5% in 0.1 M cacodylate buffer, pH 7.3). Both eyes were kept in a refrigerator (4°C) until AFM observation. In the fixed eyes, a hole was opened 6 mm behind the limbus after 40 to 50 minutes of fixation, to allow penetration of the fixative solution in the interior of the eye; the eyes were left in the fixative at least 24 hours before examination. Nonfixed specimens were examined within 1 hour of enucleation.

Before AFM observation, the anterior part of all eyes was cut away, and the cornea was freed from the underlying iris, ciliary body, and lens tissue. Triangular tissue pieces were prepared and were glued with epoxy glue to magnetic stainless steel punches, epithelium up. All preparation was performed with magnifying loops using fine forceps; special care was taken to avoid tissue wrinkling in fresh specimens and to mount specimens without applying force on the upward facing side. The preparation process lasted 5 to 10 minutes on average. Fresh and fixed specimens were observed in balanced salt solution (BSS) using the contact or the tapping AFM imaging mode.

A commercial atomic force microscope (Nanoscope III; Digital Instruments Inc., Santa Barbara, CA) including an optical viewing system, control electronics equipped with force modulation setup and piezoelectric scanners (0.8, 12, and 150 μm maximum scan range) was operated in contact force mode or oscillating contact (tapping) mode. In the contact force mode, the microscope operates by scanning a tip attached to the end of a cantilever across the sample surface; the tip contacts the sample surface during scanning. In the tapping mode the tip lightly "taps" on the sample surface during scanning contacting the surface at the bottom of its swing. (Fig. 1). All reported images were made with 512 × 512 pixels definition with typical scan rates of 1 to 5 Hz. They were processed only by flattening to remove background slope. Printouts were obtained by means of a digital color video printer (model CP-D1E; Mitsubishi, Tokyo, Japan). We used V-shaped and rectangular silicon nitride cantilevers with a spring constant of 10 to 20 mN/m (Microlever; Park Scientific Instruments, Sunnyvale, CA). To remove the contaminants, the tips were exposed to ultraviolet (UV)-ozone for 10 minutes. The UV ozone cleaning permits the removal of the hydrocarbons.[11] The force was previously adjusted for each scan image at the lowest possible value (i.e., approximately 20 pN). The measured forces after imaging were less than 100 pN.

On several specimens, surface measurements were made using the section analysis module of the AFM software. This module permits selection of one or more sections of the image and performance of various measurements, both in horizontal and vertical plane. Measurement of surface roughness by means of root mean square (RMS) value of the surface within a given area was used to quantify the unevenness of the specimen surface created by projecting structures. Surface roughness [Rq(RMS)] is defined as the SD of the Z values within the given area and is calculated using the formula:

$$Z_{\text{rms}} = \sqrt{[\sum_{i=1}^{N}(Z_i - Z_{\text{avg}})^2/N]}$$

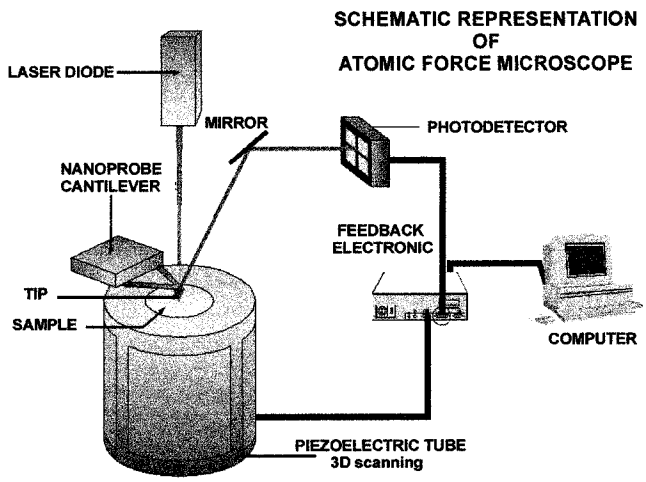

Figure 1. Operating principle of the atomic force microscope. The silicon cantilever with the integral tip operates as a force sensor. As the tip scans the specimen's surface, interaction forces between tip and specimen deflect the tip and thus the cantilever. Deflection equivalent to interactive forces (as function of tip–surface separation) is used to create three-dimensional surface topography. The translation of the deflection force into a detectable signal is usually achieved by an optical lever system. The cantilever deflection causes the incident collimated laser beam to reflect proportionally. Reflected beam is incident asymmetrically on position-sensitive photodetectors that generate electrical signals. With an appropriate feedback system, the deflection of the cantilever, and therefore the force, can be kept constant while the tip scans the specimen.

where: Z_{avg} is the average of the Z values within the given area, Z_i is the current Z values, and N is the number of points within the given area.

Results

Imaging of the epithelium was achieved for both fixed and nonfixed eyes. However, imaging was not possible in every area approached by the microscope tip. This often necessitated repeated approaches in different areas until an image of good resolution could be obtained. Adjustments of tip–specimen force, alternation of imaging mode, and replacement of microscope tip were used as necessary for successful high-resolution imaging. Very often acquisition of different magnification images in an area where a clear image had already been obtained was not possible. To obtain multiple high-quality images from different areas of the same specimen, an average of 2 to 4 hours of imaging per specimen was usually required. This prolonged examination time often resulted in the development of edema in the fresh, unprepared specimens. For this reason only images obtained within the first hour after enucleation are presented in this work. Fixed specimens, however, did not show any obvious alteration during the examination.

High-quality images were achieved within a very wide range of image magnification, from ×2000 (100 × 100 μm^2) to ×2,000,000 (100 × 100 nm^2). High-quality images were easier to obtain in medium magnification (i.e., ×20,000). Submicrometer magnifications of high resolution were obtained in only a few instances.

On fixed samples at low magnifications, AFM examination revealed the typical polygonal epithelial cells covered by nu-

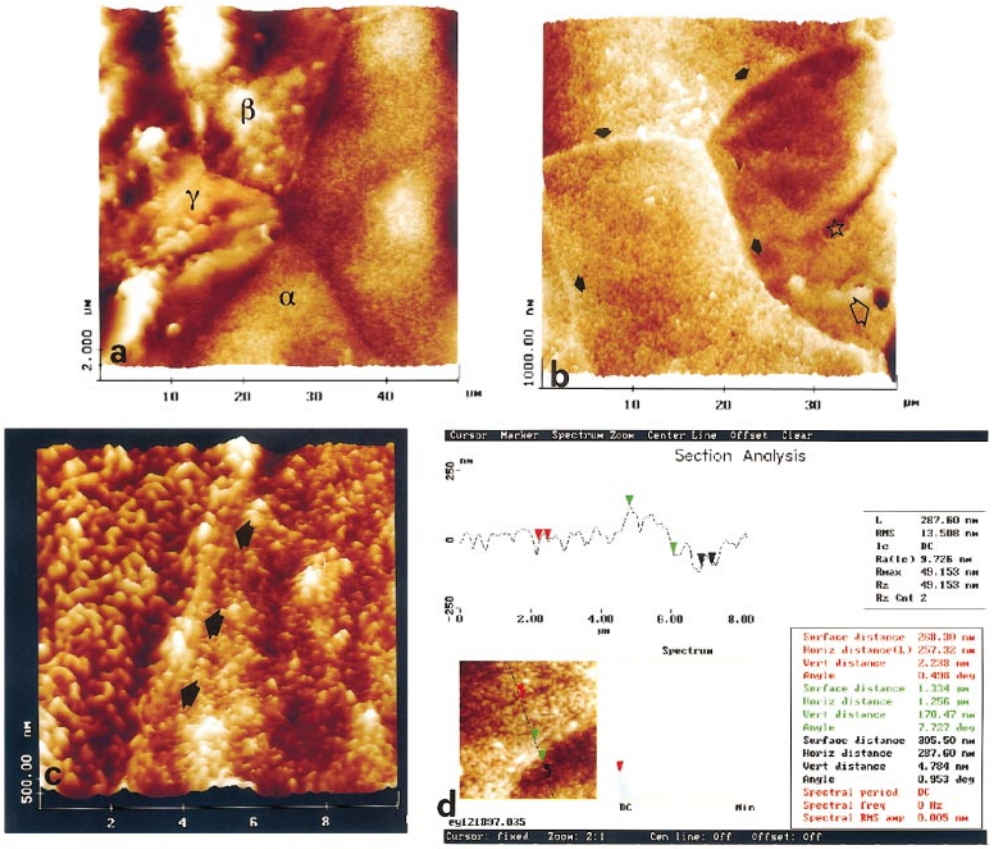

FIGURE 2. Low-force contact mode AFM imaging of corneal epithelial surface. (**a**) Low-magnification image; fixed specimen. Dark areas represent depressions of the surface whereas brighter areas are relatively higher. Parts of five cells are shown. The appearance of the surface differs characteristically among the cells. The cell in the *middle* of the *lower* part of the image (α) has a roughness between 25 and 30 nm. The roughness of the cell in the *middle* of the *upper* part of the image (β) increases to 40 to 45 nm, whereas the cell located in the *left* part of the image (γ) has a roughness of approximately 60 nm. (50-μm scan range; magnification $\times$4000; scanning force $<$100 pN. V-shaped silicon nitride cantilever, with a nominal spring constant of 10 mN/m was used). (**b**) Low-magnification image; fixed specimen. Parts of four epithelial cells can be seen. The cells are covered by microprojections. At the cell borders two parallel rows of microprojections create a ridge located relatively higher than the remaining surface (*opaque arrows*). The very bright spots on the surface may represent debris. Dark holes (*transparent arrow*) represent the characteristic craterlike structures of the epithelial cell surface. Note also the circular arrangement of the microprojections in the area indicated by the *transparent star*, creating a shallow crater. (39-μm scan range; magnification, $\times$5100; scanning force $<$100 pN). (**c**) The connection of two epithelial cells; fixed specimen. The characteristic surface microprojections of the cells are seen. The cell border consists of two parallel rows of microprojections that seem to protrude slightly over the surface (*arrows*). This appearance is typical of corneal epithelial cell borders observed by AFM. Color coding of the height makes unevenness of the cell surfaces obvious. The size and arrangement of the microprojections in the two adjacent cells look different; the microprojections in the *right* cell are more in number and finer in size. (10-μm scan range; magnification, $\times$20,000; scanning force $<$50 pN). (**d**) Section analysis of the surface of two adjacent epithelial cells; fixed specimen. Pairs of *arrows* with identical colors are used as calipers for the measurement of horizontal and vertical distances on the section determined by the *black straight line* on the image in the *lower left* part of the figure. A graph and tables are used to display the measurement results. Horizontal distances between the *red* and *black arrow* pairs in the section displayed represent the width of two microprojections, one on each cell surface (275.32, and 287.60 nm). Vertical distance between the *green* pair of *arrows* represents the difference in the hypsometric location of two areas next to the cell's border (170.47 nm).

merous characteristic microprojections. In AFM images the height of the sample surface in relation to a reference level is represented using a chromatic scale in which brighter color indicates higher location, whereas darker color indicates lower location. The three-dimensional appearance permitted a better understanding of the topographic characteristics of the sample surface. It was obvious that adjacent cells or even adjacent areas in a single cell were often located in different levels, creating bright hills and dark troughs covered by microprojections. Variations in density and size of the microprojection between adjacent cells were observed (Fig. 2a). In several instances craterlike structures could be detected on the surface of cells with low roughness. A crater's diameter ranged from 1.4 to 2.6 μm and its depth from 250 to 400 nm (Fig. 2b).

Epithelial cell connections were characteristic in AFM images: they seemed to consist of two parallel rows of microprojections, which were located at a relatively higher level compared with the adjacent cell surface, creating a ridge (Figs. 2b, 2c). The two rows were separated by a gap. In section analysis, the gap width ranged from 250 to 300 nm and its depth from 25 to 50 nm (Fig. 2d). The gap was interrupted periodically by areas where the border rows seemed to be in proximity. This pseudoperiodicity was evaluated to be between 725 nm and 1200 nm. In several instances we noted that

the ridge created by the border rows was higher if the bordering cells had different roughness.

Magnifications of ×200,000 revealed details of the morphology, orientation, and three-dimensional arrangement of microprojections. In most of these images microprojections appeared as vermiform structures. Based on their surface appearance, we could distinguish at least three types of microprojections with smooth, moderately rough, and rough surfaces. In the last two categories, the projection surface seemed to consist of many smaller roundish protruding structures (Figs. 3a, 3b, 3c). In section analysis, the microprojections were elongated in one direction with variable length; their width measured in the perpendicular direction ranged from 150 to 300 nm, and their height ranged from 20 to 120 nm. In very high-magnification images, the surface of microprojections was found to be covered by multiple fine projections ranging from 3 to 7 nm in size, most of them being 3 to 4 nm (Fig. 3d).

AFM imaging of fresh specimens was more difficult, with a higher percentage of imaging failures compared with fixed specimens. This resulted in the acquisition of a smaller number of high-resolution images from fresh samples and rendered a detailed evaluation difficult. The general characteristics of the epithelium, however, were similar to those observed in the fixed samples with microprojections covering the surface of the specimens (Figs. 3e, 3f).

The surface roughness of 70 fixed epithelial cells was measured in an effort to evaluate the distribution of roughness values. For roughness measurement we used the RMS values using 512 × 512 pixels corresponding to a reference surface of 2 × 2 μm. Based on the roughness results, we were able to distinguish at least three types of cells: smooth, moderately rough, and rough. The histogram of roughness values showed the existence of three distinct peaks that corresponded to these three cell types (Fig. 4).

Discussion

In this work we have shown that imaging of corneal epithelium is feasible using AFM. The images obtained were of high quality and in many aspects comparable to corneal epithelium images obtained by SEM in previous studies.[12] In addition, very high magnifications, usually not accessible to the SEM, were obtained.

The ability to image unprepared or minimally prepared specimens up to very high magnifications makes AFM images unique. The shrinkage of soft tissue specimens after fixation, dehydration, and critical point drying necessary for conventional SEM is well known and can cause serious artifacts, not only in compact tissues but especially in hollow tissues such as those of the eye, where the tissues are lined by delicate layers such as corneal epithelium and endothelium.[13] In this work we used both fresh unprepared corneal specimens and specimens fixed in glutaraldehyde-buffered solution. We succeeded in acquiring images of high resolution in both kinds of specimens. Submicrometer magnifications up to ×2,000,000 were achieved with very good resolution

In several cases repeated approaches in different specimen areas were necessary until a high-resolution image could be obtained. Fuzzy images were more common in fresh specimens and when submicrometer magnifications were attempted. The fuzzy character of images at submicrometer magnification was associated with difficulty of obtaining satisfying force curves and images from 800 × 800-nm scan ranges and lower. The surface of corneal epithelial cells is covered by a glycocalyx constituted of highly branched sugar residues linked to proteins that extend approximately 300 nm above the membrane surface.[14,15] We hypothesize that the fuzzy appearance of the fresh tissue surface at low magnification and the problems encountered when trying to scan submicrometer areas were linked to the presence of this glycocalyx with the sugar chains moving under the AFM tip during scanning. Similar problems have been encountered when trying to achieve very high magnification of the membrane surface of other living cells.[4] It is possible that glycocalyx interferes more with the imaging of fresh, unprepared specimens than with that of fixed specimens. Washout of most of the coating material's components by the fixative solution may be an explanation for this difference. Other investigators have found that the fixation process for conventional SEM removes most of the mucous layer that covers the normal corneal epithelium.[16,17] Future investigation using enzymatic treatment of fresh specimens may help to reveal any possible interference of glycocalyx in AFM imaging of fresh corneal epithelium.

The difficulties we encountered in imaging fresh specimens, in combination with the observation that edema developed in nonfixed specimens after some time of observation, make us believe that with the current imaging process, fixation greatly facilitates the procedure when a detailed study of the specimen is desired. The considerable time required per specimen until several high-quality images are obtained further supports this opinion. In this experiment we used a standard fixation procedure. However, because of the sensitivity of the corneal epithelium surface to the effect of drying, in future experiments installation of the fixative over the corneal surface just before enucleation may be used to minimize any drying effect during the brief period required for enucleation.

The three-dimensional topography provided by AFM offered interesting information concerning the sample surface. Differences in relative location not only between adjacent cells but also between various areas of the same cell were observed with AFM. The chromatic representation of height resulted in the appearance of bright hills and dark troughs in the specimen's surface. The number of specimens in our study does not permit the drawing of safe conclusions concerning the significance of these hypsometric differences. Our findings however are in accordance with SEM findings, in which, in low magnifications, differences in location between adjacent cells have also been described. In SEM these differences have been correlated with the age of the epithelial cells, with older cells ready to exfoliate located at a higher level.[18–20] The ability of AFM to reveal these hypsometric differences in high magnifications may permit a more detailed study and understanding of their significance.

The arrangement and morphology of epithelial microprojections were also revealed by AFM. Differences in the size, shape, and density of epithelial projections of different cells could be visualized. Based on surface roughness measurements, we could distinguish at least three types of cells with smooth, moderately rough, and rough surfaces. This categorization is in accordance with SEM findings, where three different apical epithelial cell types (dark, medium, and light) have also been described, based on cells' brightness. In SEM these

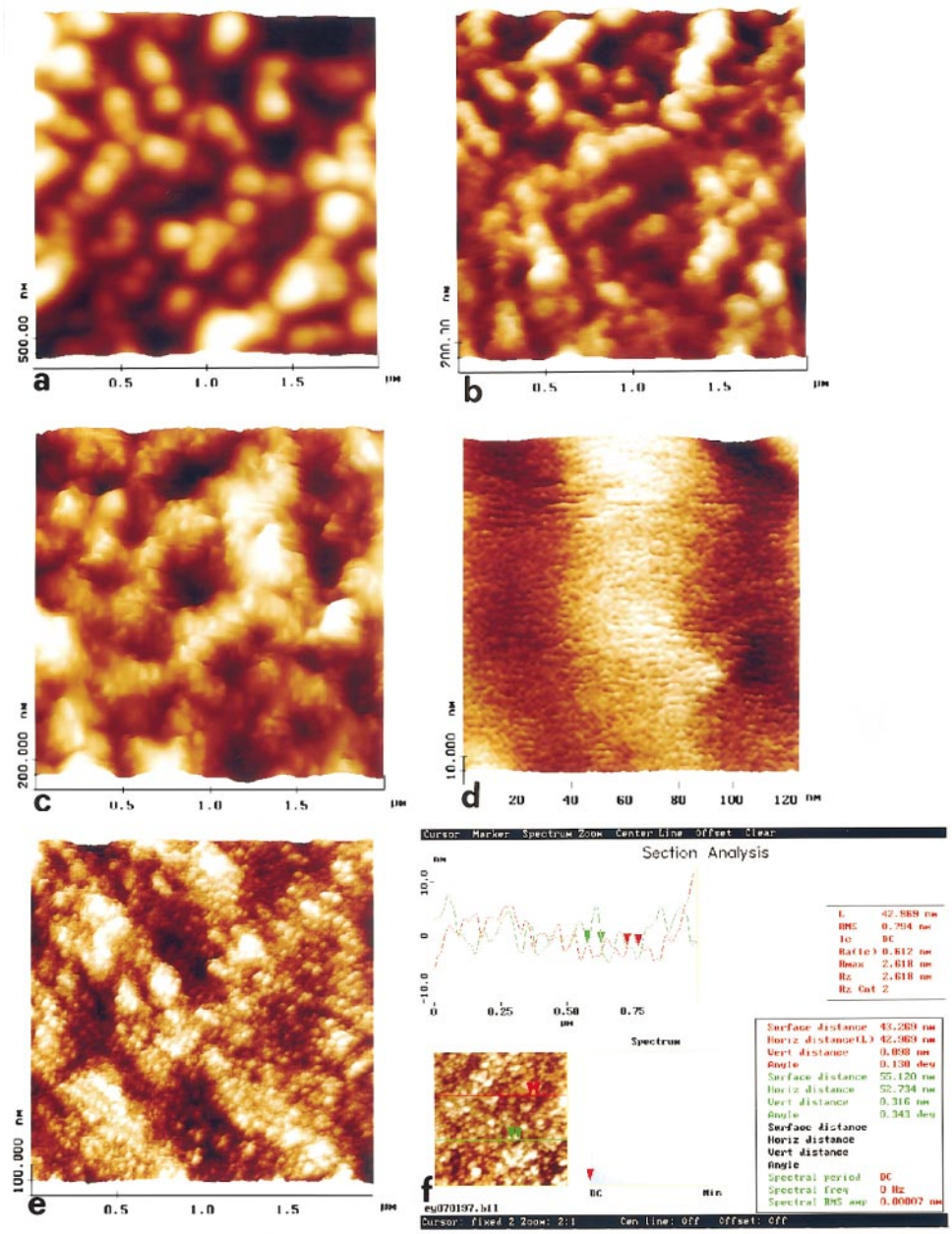

FIGURE 3. AFM imaging of corneal epithelial cell surface structures in high magnification. (**a**) High magnification of cell surface covered by smooth projections (width, ~250 nm; height, ~75 nm). Fixed specimen (2-μm scan range; magnification, ×100,000; scanning force, <50 pN). (**b**) High magnification of the cell surface covered by short projections with moderately rough surface arranged in various orientations (width, 170–300 nm; height, 24–42 nm). The projection surface seems to consist of multiple roundish, protruding structures. Fixed specimen (2-μm scan range; magnification, ×100,000; scanning force, <50 pN). (**c**) High magnification of a cell surface covered by rough projections. Further irregularity of the surface structure can be seen. Fixed specimen (2-μm scan range; magnification, ×100,000; scanning force, <50 pN). (**d**) Very high magnification of the epithelial surface. We repeatedly imaged fine particles protruding from the cell surface. These structures do not depend on the scan rate and scan angle. The particles were measured to be between 3 to 7 nm, with most of them being 3 to 4 nm. Fixed specimen (120-nm scan range; magnification, ×1,700,000; scanning force, <50 pN). (**e**) High magnification AFM image of fresh nonfixed epithelium. Microprojections covered with roundish protruding structures could be seen. Compare with Figures 3a, 3b, and 3c (2-μm scan range; magnification, ×100,000; scanning force, <50 pN). (**f**) Section analysis of fresh nonfixed epithelium. Two roundish protruding structures are measured in two different sections, 42.96 and 52.73 nm in diameter (1-μm scan range; magnification, ×200,000; scanning force, <50 pN).

differences have been correlated with variations in density of surface microplicae and with the cell's age: Light cells are considered young, whereas dark cells are thought to be ready to exfoliate.[18–20] A possible correlation may be that light, medium, and dark cells in SEM correspond to smooth, moderately rough, and rough cells in AFM, respectively. Further investigation is necessary to determine whether such a correlation exists. The characteristic craters at the epithelial cell surface that have been described with SEM[21] were also imaged in AFM, especially in cells with low roughness. Using the

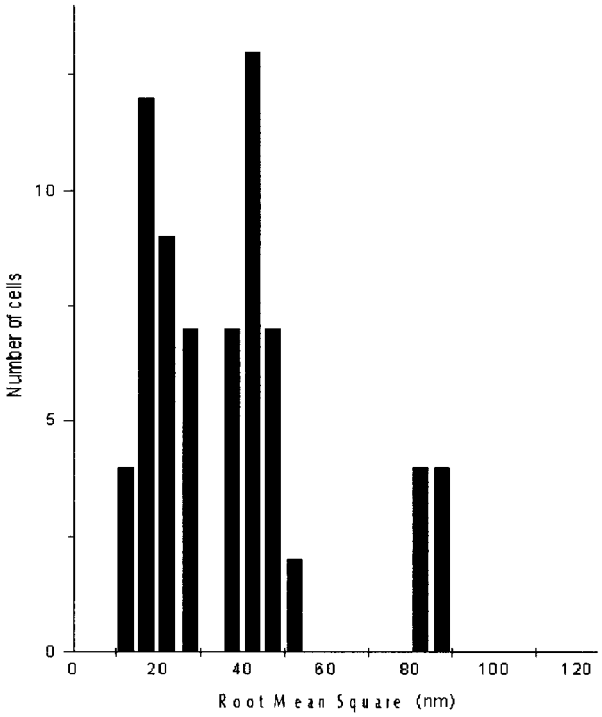

FIGURE 4. Histogram of surface roughness values of 70 fixed corneal epithelial cells measured by means of the RMS value of the surface within a given area. Three distinct peaks can be seen, corresponding from left to right to smooth, moderately rough, and rough cells.

section analysis module of the microscope we were able to measure both the diameter and the depth of these structures.

A characteristic arrangement of the microprojections in two parallel rows at epithelial cell borders was seen in all our specimens. With AFM we were able to identify and measure a gap between the two rows. We also identified areas where the two rows were in proximity; these areas may correspond to tight junctions that are known to surround the apical epithelial cell circumference near the apical margin.[22] The projections' arrangement at the cell borders may reflect the organization of the supporting cytoskeleton fibrils at the level of the superficial intercellular contacts.

At high magnifications, the microprojections had a vermiform appearance and, based on their surface roughness, we could identify at least three types of them: smooth, moderately rough, and rough. In specimens where submicrometer magnifications were achieved it was obvious that microprojection surface was covered throughout by multiple, fine, projecting particles with lateral sizes ranging between 3 and 7 nm. These structures may represent the appearance of the molecular structure of the outer membrane of the epithelial cells. In previous experiments similar structures have been described on the surface of MDCK cells and of red blood cells and have been correlated to proteins exposed at the membrane's surface.[4,23]

Profile measurements represent a valuable utility of AFM. Section analysis enabled performance of detailed measurements of all selected structures, both in horizontal and vertical plans. Measurements of difference in relative cell location, depth of epithelial craters, and depth of the gap between the border rows were achieved. This option facilitates easy three-dimensional measurements of the observed structures, something not available in conventional scanning microscopy. In addition the software analysis permits quantitative characterization of the surface roughness. In this work the surface roughness was measured using the root mean square heights within a given area and based on roughness values, we were able to demonstrate the existence of three cell types. The number of cells measured, however, is relative small. The application of these measurements in a larger number of cells is necessary to strengthen the statistical significance of our findings. In addition, it must be mentioned that surface roughness can also be described using parameters such as the ratio of height to the characteristic horizontal dimensions of the projecting structures of the surface. Such approaches should be used in future studies for more detailed measurements of surface roughness.

Another unique characteristic of AFM is its ability to measure various micromechanical properties of the specimens such as surface friction, elasticity, and viscosity.[1,2] Currently, we are analyzing images representing the topographic distribution of friction on the surface of our specimens. This information is quite new and seems impressive. It is possible that information concerning the micromechanical properties of the cell surface can act complementarily to traditional morphologic information and expand the range of applications of scanning microscopy. Additional investigation, however, is needed to determine its clinical significance. It must also be emphasized that for such measurements to have validity, they would have to be made on fresh tissue.

In conclusion, our experiment strongly suggests that AFM represents a new powerful tool for the imaging of the corneal epithelial surface. Minimal tissue preparation, high (submicrometer) magnifications, and the capability of easy quantification of observed structures represent some of its unique characteristics. In this work we defined the AFM imaging parameters appropriate for corneal epithelium and obtained high quality images of this tissue. In general our findings with AFM in this relatively small number of specimens support the findings of previous SEM studies of corneal epithelium. In addition, it became obvious that there is new, interesting information to be obtained with AFM that merits further investigation. The application of AFM imaging in other ophthalmic tissues should also be studied in the future.

Acknowledgments

The authors thank Irini Naoumidi for her helpful remarks.

References

1. Radmacher M, Tillman RW, Fritz M, Gaub HE. From molecules to cells: imaging soft samples with the atomic force microscope. *Science.* 1992;257:1900–1905.
2. Ratneshwar L, Scott AJ. Biological applications of atomic force microscopy. *Am J Physiol.* 1994;266:C1–C21.
3. Hansma HG, Vesenka J, Siegerist C, et.al. Reproducible imaging and dissection of plasmid DNA under liquid with atomic force microscope. *Science.* 1992;56:1180–1184.
4. Le Grimellec C, Lesniewska E, Cachia C, Schreiber JP, Goudonnet JP. Imaging of the membrane surface of MDCK cells by atomic force microscopy. *Biophys J.* 1994;67:36–41.
5. Le Grimellec C, Lesniewska E, Giocondi MC, Cachia C, Schreiber JP, Goudonnet JP. Imaging of the cytoplasmic leaflet of the plasma

membrane by atomic force microscopy. *Scanning Microsc.* 1995;9: 401–411.
6. Lesniewska E, MC Giocondi, Vie V, Finot E, Goudonnet JP, Le Grimellec C. Atomic force microscopy of renal cells: limits and prospects. *Kidney Int.* 1998;65:42–48.
7. Allison DP, Kerper PS, Doktycz MJ, et al. Mapping individual cosmid DNAs by direct AFM imaging. *Genomics.* 1997;41:379–384.
8. Hoh JH, Lal R, John SA, Revel JP, Arndorf MF. Atomic force microscopy and dissection of gap junctions. *Science.* 1991;253: 1405–1406.
9. Fullwood NJ, Hammiche A, Pollock HM, Hourston DJ, Song M. Atomic force microscopy of the cornea and sclera. *Curr Eye Res.* 1995;14:529–535.
10. Meller D, Peters K, Meller K. Human cornea and sclera studied by atomic force microscopy. *Cell Tissue Res.* 1997;288:111–118.
11. Thundat T, Zheng X-Y, Chen GY, Warmack RJ. Role of relative humidity in atomic force microscopy imaging. *Surface Sci Lett.* 1993;294:939–943.
12. Pfister RR. The normal surface of corneal epithelium: a scanning electron microscopic study. *Invest Ophthalmol.* 1973;12:654–68.
13. Virtanen J, Uusitalo H, Palkama A, Kaufman H. The effect of fixation on corneal endothelial cell dimensions and morphology in scanning electron microscopy. *Acta Ophthalmol.* 1984;62:577–585.
14. Gipson IK, Yankauchas M, Spurr–Michaud SJ, et al. Characteristics of a glycoprotein in the ocular surface glycocalyx. *Invest Ophthalmol Vis Sci.* 1992;33:218–227.
15. Nichols B, Dawson CR, Tongi B. Surface features of the conjunctiva and cornea. *Invest Ophthalmol Vis Sci.* 1983;24:570–576.
16. Hazlett L, Dudzik D, Harries B. Development of ocular mucin: scanning EM analysis. *Ophthalmic Res.* 1986;18:28–33.
17. Nichols BA, Chiappino ML, Dawson CR. Demonstration of the mucous layer of the tear film by electron microscopy. *Invest Ophthalmol Vis Sci.* 1985;26:464–473.
18. Doughty MJ. Morphometric analysis of the surface cells of rabbit corneal epithelium by scanning electron microscopy. *Am J Anat.* 1990;189:316–328.
19. Versura P, Bonvicini F, Caramazza R, Laschi R. Scanning electron microscopy study of human cornea and conjunctiva in normal and various pathological conditions. *Scanning Electron Microsc.* 1985; 4:1695–1708.
20. Doughty MJ. The cornea and corneal endothelium in aged rabbit. *Optom Vis Sci.* 1994;71:809–818.
21. Pfister R, Renner M. The histopathology of experimental dry spots and dellen in the rabbit cornea: a light microscopy and scanning and transmission electron microscopy study. *Invest Ophthalmol Vis Sci.* 1977;16:1025–1038.
22. McLaughlin B J, Cadwell RB, Sasaki Y, Wood TO. Freeze-fracture quantitative comparison of rabbit corneal epithelial and endothelial membranes. *Curr Eye Res.* 1985;4:951–961.
23. Hoerber JKH, Haberle W, Ohnesorge F, et al. Investigation of living cells in a nanometer regime with the scanning force microscope. *Scanning Microsc.* 1992;6:919–930.